Progress In Electromagnetics Research M, Vol. 51, 101–111, 2016

Assessment of Materials for High-Speed PMSMs Having a Tooth-Coil Topology

Nikita Uzhegov[1, *], Nikolai Efimov-Soini[2], and Juha Pyrhönen[1]

Abstract—In this paper, materials frequently used in high-speed (HS) electrical machines are assessed. High-speed permanent magnet synchronous machines with a special tooth-coil topology serve as an example for the assessment. The lamination and rotor sleeve materials are compared taking into account their price, per unit losses, resistivity, and other factors. The resulting tables provide the electrical machine designer with a means to enhance the HS machine performance at low costs.

1. INTRODUCTION

According to the increasing number of publications on the topic [1–3], the interest of the research community in high-speed (HS) electrical machines is growing. The multidisciplinary nature of the HS electrical machine design procedure attracts researchers from the fields of electromagnetics, thermal analysis, rotordynamics, power electronics, material science as well as bearing designers [4–8]. Intensive studies in the field are motivated by the industry's interest in these machines. Application fields of HS machines cover water treatment, energy sector, heating, ventilation, and air conditioning (HVAC), and food industry. The advantages of HS motors and generators have made these machines attractive in various application fields. These advantages are a higher system efficiency, a smaller carbon footprint and system size, and a higher power density compared with conventional rotating electrical machines [9].

High-speed induction machines (HSIM) and permanent magnet synchronous machines (PMSM) are the most attractive and widespread solutions in the industry. The HS PMSM provides a higher efficiency and power density and a higher power factor than the HSIM, especially in low-power applications [10, 11].

In this paper, a special HS PMSM topology is considered. The machines under study have six stator slots and nonoverlapping concentrated windings, that is, tooth-coil (TC) windings. The rotor has two poles and consists of a full cylindrical permanent magnet (PM) and a retaining sleeve around the PM. The advantages of this topology are the simple rotor and stator construction and assembly process, a high efficiency and power factor, a sinusoidal back-EMF shape, and a short axial protrusion length of the end windings. The short end windings allow to achieve a short rotor length, which, in turn, increases the maximum rotational speed [12, 13].

A low number of poles is preferable in high-speed machinery because of the converter limitations and a significant increase in some loss components at high nominal frequencies [14]. In the case of a 2-pole HS PMSM with distributed windings (DW), the axial protrusion length of the end windings can be equal to the stator active length. Therefore, the rotor is longer, which further complicates the design of the drive train. This problem can be avoided by using tooth-coil windings. However, there are several factors that limit the adoption of the proposed topology with TC windings.

This paper describes some design solutions aimed to increase the power or rotational speed of the HS PMSM having the above-mentioned topology. The effects of the selection of the stator and rotor

Received 6 August 2016, Accepted 18 October 2016, Scheduled 28 October 2016

* Corresponding author: Nikita Uzhegov (nikita.uzhegov@lut.fi).

[1] Department of Electrical Engineering, School of Energy Systems, Lappeenranta University of Technology (LUT), Lappeenranta 53851, Finland. [2] Department of Operation Management and Systems Engineering, School of Business and Management, LUT, Lappeenranta 53851, Finland.

materials on the machine performance and costs are presented. The design solutions are elaborated on and compared with each other by two analyses.

There are various methods to assess an engineering system design; however, only a few of them are widely used in the industry [15]. This paper focuses on two popular methods, namely, the Pugh matrix and the Analytical Hierarchical Process (AHP).

The main contribution of this paper is the description of materials enabling a higher power or rotational speed of HS machines and a comparison of these materials with each other. This information will facilitate material selection based on the performance/complexity ratio. The data are validated by prototypes constructed and measured in the study. The proposed methods of comparison can be applied to other design optimization options and other electrical machine types.

2. CONSTRUCTION AND KEY LIMITATIONS

The design of any high-speed electrical machine is a multidisciplinary process owing to the mechanical, thermal, and electromagnetic aspects to be taken into account simultaneously. In the case of HS electrical machines, the electromagnetic design is more complicated than with conventional machines. After the electromagnetic design is completed, a detailed thermal and rotordynamic analysis must be performed. If any of the boundaries is not met, a new round of iteration starts.

This paper proposes a material selection strategy that can help to overcome the boundaries set by the thermal, mechanical, and electromagnetic limitations. An HS electrical machine topology serves as an example to demonstrate the influence of every design solution in detail. Two prototypes based on the proposed topology were constructed and measured. In these machines, alternative design approaches were adopted to overcome the limitations. These methods of comparison can also be applied to any other electrical machines.

The topology under consideration is aimed to reduce the manufacturing costs. To this end, there are only six stator slots in the topology. The rotor consists of a full cylindrical diametrically magnetized PM inside a retaining sleeve. Fig. 1 illustrates the cross-section of the HS topology with an example of the flux lines, flux distribution, and winding scheme. The Finite Element Method (FEM) calculations of the machines were performed using the Cedrat Flux software package. All calculations were made in 2D; however, the 3D effects were taken into account using the method described in [16]. A detailed description of the FEM design process of the tooth-coil machine topology can be found in [17].

The structural limitations of the topology are mainly related to the stresses between the retaining sleeve and the magnet. These stresses are caused by centrifugal forces and thermal expansion. The contact between the PM and the retaining sleeve must be maintained from zero up to the maximum allowed rotational speed and at any operating temperature. Simultaneously, the stresses between the

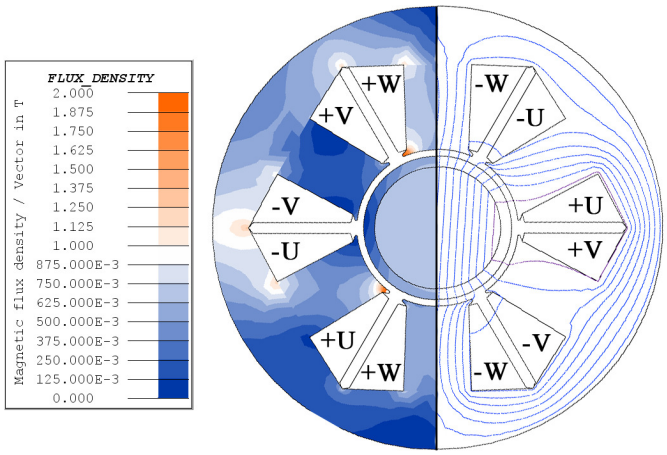

Figure 1. Cross-section of the tooth-coil topology under investigation. The rated point flux density and flux line distribution are shown in the example machine. The winding scheme is demonstrated.

PM and the sleeve must be below the yield strength of the retaining sleeve material taking into account the safety factor [18].

The maximum length of the machine is associated with the rotordynamics. Usually, the drive system is designed to be undercritical. However, there are bearing solutions that allow overcritical operation. In the topology under consideration, the rotordynamics is usually not a critical limitation. Because of the TC windings, the total rotor length is significantly shorter than with a DW machine of a similar performance. The shorter rotor enables undercritical operation in most of the cases with the topology under study.

The losses place significant limitations both on the rotor and stator parts. The rotor losses consist of magnet and retaining sleeve losses caused by eddy currents. Further, about three-quarters of the total rotor losses occur in the conducting retaining sleeve material. The total rotor losses do not significantly reduce the machine efficiency, but they can cause permanent magnet overheating and ultimately, irreversible demagnetization.

The stator core losses are a limiting factor at high operating frequencies. Reliable loss data at high frequencies are required to adjust the coefficients of the applied hysteresis loss model and calculate the core losses at the nominal frequency by the FEM.

In this topology, copper losses can be very high, because the winding factor is only 0.5. In the winding design, it is extremely important to limit extra copper losses, including losses caused by the skin effect and circulating currents. An analysis of the prototypes has shown that the rotor and end winding temperatures are the two main thermally critical factors. These temperatures can be selected as the key indicators of whether the current design meets the boundary conditions.

Mechanical losses start to play a significant role at high rotational speeds. Because of the smooth outer rotor surface and a relatively small rotor diameter, friction and windage losses are not a limiting factor. In the case of ball, air film, or fluid film bearings, bearing losses constitute the majority of the mechanical losses in the topology under analysis. The frequency converters may be a limiting factor at high frequencies even in two-pole machines. To minimize the losses in the machine, various converter topologies, sampling techniques, and switching frequencies are used [19, 20].

There are various alternatives to overcome the above-mentioned multidisciplinary limitations and achieve a better performance with the topology presented in this paper. These solutions require diverse resources at the design and manufacturing stages and yield different results. The following section introduces methods that allow to compare alternative solutions and rank them. By applying the results of this comparison, design engineers are able to select the most promising materials.

3. ASSESSMENT METHODS

Two methods are frequently applied to the design assessment: the Pugh matrix [21] and the Analytical Hierarchical Process (AHP) [22]. The AHP is used for concept ranking and the Pugh matrix for pairwise comparison.

In the Pugh matrix method, the concepts are compared with the "datum" concept with respect to several parameters. Thus, a value "better than datum," "worse than datum," or "similar" is determined for each parameter. The best design has the highest number of "better than datum" values. This method is widely used in various areas, for example, in energy and mechanical engineering, and it can also be integrated with other methods such as the Quality Function Deployment (QFD) [23–26].

The AHP is a method developed by Professor T. L. Saaty in 1977, and it is based on the decomposition of the main problem into subproblems. The method consists of two main phases: ranking of the evaluation criteria and assessment of the design. In order to achieve the goal, pairwise comparisons of all criteria are carried out to determine the relative importance of each criterion. Next, pairwise comparisons are made between all alternatives separately for each criterion. Based on these comparisons, an overall selection is made. Eigenvalues and eigenvectors are used to ensure that the decision maker's judgments are consistent [27]. This method is used for electrical machine design [28], measurement system development [29], and electrical energy generation planning [30, 31].

A fair comparison of diverse parameters can be made by using normalized data. For normalization,

the following formulas are used:

$$f_{\text{norm}} = \begin{cases} \dfrac{f_{\text{initial}} - f_{\min}}{f_{\max} - f_{\min}} - \text{ if } f_{\max} \text{ is the best value,} \\ 1 - \dfrac{f_{\text{initial}} - f_{\min}}{f_{\max} - f_{\min}} - \text{ if } f_{\max} \text{ is the worst value,} \end{cases} \tag{1}$$

where f_{norm} is the normalized result, f_{initial} the initial value, and $f_{\max}$ and $f_{\min}$ are the maximum and minimum values of this parameter.

By this approach, the normalized data can be interpreted in equal terms. For each parameter, 0 is the worst result and 1 is the best result.

4. HIGH-SPEED ELECTRICAL MACHINE MATERIALS

4.1. Assessment of the Stator Material

The methods introduced in this paper are demonstrated for the selection of the stator lamination material. The most commonly used lamination materials in high-speed machines are selected for comparison, namely M270-50A, M270-35A, NO27, NO20, NO10, and a more rare 10JNEX900 lamination. Ten lamination suppliers were requested for a quotation for the same prototype geometry and alternative materials available. Based on the quotations, the relative costs and availability of the materials are obtained. These parameters are given in Table 1. The other important parameters are obtained from the manufacturers' datasheets [32, 33]. These parameters include the relative losses at 400 Hz and 2500 Hz at 1 T. The space factor depends on the lamination and insulation thickness and has an impact on the core losses. The relative values of this parameter are listed according to [34, 35] in Table 1. The value of the flux density at which the flux density saturation occurs at 50 Hz is shown with the relative parameter saturation. The relative resistivity and yield strength of the lamination materials are also presented. The data are normalized using (1).

Table 1. Normalized parameters of the stator lamination material.

Material	Price	Availability	Loss at 400 Hz	Loss at 2500 Hz	Space factor	Saturation	Resistivity	Yield strength
M270-50A	1	1	0	0	1	0.22	0.64	0.33
M270-35A	0.89	0.88	0.39	0.52	0.86	0.11	0.64	0.26
NO27	0.78	0.63	0.57	0.70	0.57	0	1	0.19
NO20	0.72	0.38	0.66	0.80	0.29	0.78	0.36	0
NO10	0.61	0.25	0.66	0.96	0	0	0.36	0
10JNEX900	0	0	1	1	0	1	0	1

Table 2. Comparison matrix of the stator lamination material parameters.

Parameters	Price	Availability	Loss at 400 Hz	Loss at 2500 Hz	Space factor	Saturation	Resistivity	Yield strength
Price	1	2	1	2	3	4	4	6
Availability	1/2	1	1	2	3	3	2	4
Loss at 400 Hz	1	1	1	3	2	3	3	5
Loss at 2500 Hz	1/2	1/2	1/3	1	1/2	1	1/4	2
Fill factor	1/3	1/3	1/2	2	1	2	1/4	2
Saturation	1/4	1/3	1/3	1	1/2	1	1/4	1
Resistivity	1/4	1/2	1/3	4	4	4	1	4
Yield strength	1/6	1/4	1/5	1/2	1/2	1	1/4	1

Table 3. Weight coefficients of the stator lamination material parameters.

Parameters	Weight coefficient	Parameter rank
Price	0.253	1
Availability	0.169	3
Loss at 400 Hz	0.204	2
Loss at 2500 Hz	0.063	6
Fill factor	0.077	5
Saturation	0.048	7
Resistivity	0.148	4
Yield strength	0.037	8

Table 4. Ranking results of the stator lamination material.

Parameters	Ranking factor	Rank
M270-50A	0.616	3
M270-35A	0.621	2
NO27	0.622	1
NO20	0.564	4
NO10	0.434	5
10JNEX900	0.425	6

After the data normalization, the AHP method starts the pairwise comparison of the material properties. The importance of price in the material selection is compared first with availability, then with losses at 400 Hz, and with all other properties. For example, in Table 2, a judgment is made that for an HS machine, the material price is twice as important as availability (thus the value 2 in the table cell). The relative importance of one parameter over another is expressed. The same procedure is applied for all material parameters. All the judgments constitute an $n \times n$ pairwise comparison matrix, where the main diagonal elements equal 1 and $a_{ij} = 1/a_{ji}$ for all $i, j = 1, \ldots, n$. An example of the comparison matrix for the lamination parameters is shown in Table 2.

The next step is the conversion of the comparison matrix in Table 2 into weight coefficients for every parameter. For this purpose, an eigenvector is calculated. The values of the eigenvector are the relative weight coefficients of the parameters. The weight coefficients and ranks of the lamination material parameters are given in Table 3. According to the results, price, loss at 400 Hz, and availability are the most important parameters for the selected operating frequencies.

The final step is scoring of the results based on the data of Tables 2 and 3. The resulting ranking factors RF are calculated by the following equation

$$\mathrm{RF} = \sum_{i=1}^{n} f_i w_i, \tag{2}$$

where f_i are the material normalized parameters and w_i the weight coefficients of the parameters. The calculated ranking factors and the ranks for the lamination materials are given in Table 4. The results show that NO27, M270-35A, and M270-50A are the first options for the design. These materials have an acceptable per unit loss level at 400 Hz and a low price, and are usually available in stock according to the data of Table 1.

Sometimes in the design process there is a need to select between two lamination material options. A pairwise comparison applying the Pugh matrix allows to choose one out of two materials based on their parameters. The method has three steps. First, one option is selected and assigned as a basis or "datum" for the comparison. The second step is the comparison of the parameters of the options with

Table 5. Comparison of the Datum material NO20 and M270-50A.

Parameters	NO20	M270-50A	Result
Price	0.72	1	better than datum (+)
Availability	0.25	1	better than datum (+)
Loss at 400 Hz	0.66	0	worse than datum (−)
Loss at 2500 Hz	0.8	0	worse than datum (−)
Fill factor	0.29	1	better than datum (+)
Knee	0.78	0.22	worse than datum (−)
Resistivity	0.36	0.64	better than datum (+)
Yield strength	0	0.33	better than datum (+)

Table 6. Pugh matrix for the stator lamination material.

Material \ Datum	M270-50A	M270-35A	NO27	NO20	NO10	10JNEX900
M270-50A		5 (+) 2 (-) 1 (=)	5 3 0	5 3 0	6 2 0	4 4 0
M270-35A	2 (+) 5 (-) 1 (=)		5 3 0	5 3 0	6 2 0	4 4 0
NO27	3 (+) 5 (-) 0 (=)	3 5 0		5 3 0	5 2 1	4 4 0
NO20	3 (+) 5 (-) 0 (=)	3 5 0	3 5 0		4 2 2	4 4 0
NO10	2 (+) 6 (-) 0 (=)	2 6 0	2 5 1	2 4 2		3 4 1
10JNEX900	4 (+) 4 (-) 0 (=)	4 4 0	4 4 0	4 4 0	4 3 1	

a datum. Finally, the next option is assigned as a datum, and the procedure is repeated.

For example, the material NO20 is assigned as a datum and compared with M270-50A. The results of the comparison are shown in Table 5. The pairwise comparison shows that M270-50A has five parameters that are better than the datum, and three parameters that are worse than the datum. According to the Pugh method, the material M270-50A is a better option than NO20. This is also confirmed by the AHP analysis, where M270-50A has a rank of 3 and NO20 has a rank of 4.

Table 6 shows the results of the pairwise material comparison based on the Pugh method. The rows represent the selected materials, which are compared with respect to the datum, and the columns represent the datum. In each cell, the top value indicates the number of parameters that are better than the datum, the middle value is the number of parameters that are worse than the datum, and the bottom value is the number of parameters of equal value. If the selected material is better than the datum, the cell is highlighted in green, if it is worse than the datum, the cell is highlighted in red, and if the materials are equal, the cell is highlighted in yellow.

The drawback of the Pugh method is the equal assessment of all option parameters. Therefore, less important parameters, for instance, lamination yield strength, may affect the results of the pairwise comparison. It can be seen in Table 6 that by applying the Pugh method it is difficult to compare materials that have very distinct parameters, for example, 10JNEX900. Therefore, the Pugh method is suitable for the comparison of options that have similar parameters.

When assessing the lamination materials by the two methods described above, it can be seen that the price difference is not critical in the case of the M-series and NO-series steels; however, the availability of these series is usually an issue. In many cases, NO20 and higher grades have to be purchased separately. Because of the exceptional characteristics of the 10JNEX900, this material has the lowest per unit losses at high frequencies among silicon-iron (SiFe) alloys [33]. The high price and low availability of this material makes it a favorable choice only in very demanding applications.

4.2. Assessment of the Rotor Sleeve Material

The rotor sleeve material significantly affects the maximum power and rotational speed of the proposed HS machine topology. The electromagnetic, mechanical, and thermal factors are acting simultaneously on the retaining sleeve. The common rotor retaining sleeve materials used in HS PMSMs and their normalized properties are given in Table 7. The materials prices and availability are obtained by the same procedure as with the stator lamination. The yield strength, density, thermal conductivity, and resistivity of the sleeve materials are found in [36–38].

Similar to the stator lamination AHP analysis, a comparison matrix is produced for the rotor lamination materials. The comparison matrix of the material parameters is shown in Table 8. The eigenvector of this matrix provides information about the relative importance of each parameter. The weight coefficients of the rotor retaining sleeve material parameters are shown in Table 9.

The yield strength and density of the material determine the maximum rotational speed, while resistivity defines the losses in the retaining sleeve. Therefore, these parameters are of a high importance. A high yield strength allows higher rotational speeds than a low material density, which is shown in Table 8 with the value of 5. The price and availability of the materials should also be taken into account in the selection of the rotor sleeve material.

According to the AHP method results presented in Table 10, the titanium retaining sleeve is the best compromise between cost and performance. Stainless steel or carbon fiber retaining sleeves are the next best options depending on the stresses occurring in the sleeve material.

Table 7. Normalized parameters of the rotor retaining sleeve material.

Material	Price	Availability	Yield strength	Density	Thermal conductivity	Resistivity
ANSI 316L	1	1	0	0.03	1	0
Ti6Al4V	0.64	0.43	0.75	0.59	0.38	0.04
Inconel 718	0	0	1	0	0.69	0.02
Carbon fiber	0.21	0	0.66	1	0	1

Table 8. Comparison matrix of the rotor retaining sleeve material parameters.

Parameters	Price	Availability	Yield strength	Density	Thermal conductivity	Resistivity
Price	1	2	1/2	3	2	1
Availability	1/2	1	1/3	3	2	3/2
Yield strength	2	3	1	5	5/2	2
Density	1/3	1/3	1/5	1	1/3	1/5
Thermal conductivity	1/2	1/2	2/5	3	1	1/2
Resistivity	1	2/3	1/2	5	2	1

Table 9. Weight coefficients of the rotor retaining sleeve material parameters.

Parameters	Weight coefficient	Parameter rank
Price	0.192	2
Availability	0.157	4
Yield strength	0.326	1
Density	0.048	6
Thermal conductivity	0.103	5
Resistivity	0.174	3

Table 10. Ranking results of the rotor retaining sleeve material.

Material	Ranking factor	Rank
ANSI 316L	0.45	2
Ti6Al4V	0.51	1
Inconel 718	0.34	4
Carbon fiber	0.44	3

Table 11. Pugh matrix for the rotor retaining sleeve material.

Material \ Datum	ANSI 316L	Ti6AI4V	Inconel 718	Carbon fiber
ANSI 316L		3 (+) 3 (-) 0 (=)	4 2 0	3 3 0
Ti6AI4V	3 (+) 3 (-) 0 (=)		4 2 0	4 2 0
Inconel 718	2 (+) 4 (-) 0 (=)	2 4 0		2 4 0
Carbon fiber	3 (+) 3 (-) 0 (=)	2 4 0	4 2 0	

Table 11 shows the Pugh matrix for the retaining sleeve materials. The data are obtained applying the principle explained in Table 5. In line with the AHP method results, the Pugh matrix demonstrates that Inconel is the least favorable option because of its high price.

The suggested stainless steel grades are the lowest-cost options, and these materials have the lowest yield strengths and the highest conductivities compared with the other sleeve materials. The implementation of titanium, Inconel, or carbon fiber significantly extends the boundaries of the machine with the proposed topology but also the material price rises. Carbon fiber has exceptional yield strength and resistivity but its thermal conductivity is very low. In the proposed construction, this is critical because the only rotor cooling channel is the outer surface of the sleeve. In this case, the carbon fiber can only be selected with permanent magnets of high temperature grade.

5. PROTOTYPE VALIDATION

Based on the results of the material analysis, two prototypes with the proposed topology were built and optimized. The first one is a 3.5 kW, 45 000 rpm PMSM for a turbo blower. The second one is an 11 kW, 31 200 rpm permanent magnet synchronous generator for a micro Organic Rankine Cycle (ORC) power plant.

In the 3.5 kW machine, NO10 lamination and a titanium retaining sleeve were used. These materials were chosen to significantly extend the speed and power limits and ensure stable operation of the first prototype. The other design methods implemented in the machine were installation of magnetic wedges and selection of the bearing solution.

Another approach to the electrical machine design was taken in the 11 kW generator. The materials chosen for the second prototype were M-270-35A lamination and an ANSI 316L retaining sleeve. According to Tables 4 and 10, these materials are preferable solutions. The methods applied in the design process are optimization of the air gap length, yoke thickness, and tooth tip, and installation of a magnetic wedge. As a result, the performance of the 11 kW machine is relatively similar to the 3.5 kW machine but with lower costs and manufacturing time.

The prototype test results show a good correlation between the simulated and measured losses. More detailed information of the prototypes and testing can be found in [39].

6. CONCLUSION

In this paper, an assessment of the lamination and rotor sleeve materials for a 2-pole, 6-slot HS PMSM with tooth-coil windings is presented. The materials are assessed applying the AHP and Pugh matrix methods. The rank results of the AHP assessment are presented in tables. The Pugh matrix allows a pairwise comparison of the selected materials for high-speed electrical machines.

Two prototypes demonstrate alternative strategies for the HS machine design. In the 3.5 kW machine, expensive materials are used to extend the power and speed limits of the machine. In the case of the 11 kW machine, only the materials with the highest assessment ranks are applied to the design.

REFERENCES

1. Chau, K.-T., W. Li, and C. H. T. Lee, "Challenges and opportunities of electric machines for renewable energy," *Progress In Electromagnetics Research B*, Vol. 42, 45–74, 2012.
2. Misron, N. B., S. Rizuan, R. N. Firdaus, C. Aravind Vaithilingam, H. Wakiwaka, and M. Nirei, "Comparative evaluation on power-speed density of portable permanent magnet generators for agricultural application," *Progress In Electromagnetics Research*, Vol. 129, 345–363, 2012.
3. Gerada, D., A. Mebarki, N. Brown, C. Gerada, A. Cavagnino, and A. Boglietti, "High-speed electrical machines: Technologies, trends, and developments," *IEEE Transactions on Industrial Electronics*, Vol. 61, No. 6, 2946–2959, Jun. 2014.
4. Pyrhönen, J., J. Nerg, P. Kurronen, and U. Lauber, "High-speed high-output solid-rotor induction-motor technology for gas compression," *IEEE Transactions on Industrial Electronics*, Vol. 57, No. 1, 272–280, Jan. 2010.
5. Touati, S., R. Ibtiouen, O. Touhami, and A. Djerdir, "Experimental investigation and optimization of permanent magnet motor based on coupling boundary element method with permeances network," *Progress In Electromagnetics Research*, Vol. 111, 71–90, 2011.
6. Riemer, B., M. Lessmann, and K. Hameyer, "Rotor design of a high-speed permanent magnet synchronous machine rating 100,000 rpm at 10 kw," *Proc. IEEE ECCE*, 3978–3985, Sep. 2010.
7. Jiang, W. and T. Jahns, "Coupled electromagnetic-thermal analysis of electric machines including transient operation based on finite-element techniques," *IEEE Transactions on Industry Applications*, Vol. 51, No. 2, 1880–1889, Mar. 2015.
8. Pesch, A., A. Smirnov, O. Pyrhönen, and J. Sawicki, "Magnetic bearing spindle tool tracking through m-synthesis robust control," *IEEE ASME Transactions on Mechatronics*, Vol. 20, No. 3, 1448–1457, Jun. 2015.

9. Bianchi, N., S. Bolognani, and F. Luise, "Potentials and limits of high-speed PM motors," *IEEE Transactions on Industry Applications*, Vol. 40, No. 6, 1570–1578, Nov. 2004.
10. Kolondzovski, Z., A. Arkkio, J. Larjola, and P. Sallinen, "Power limits of high-speed permanent-magnet electrical machines for compressor applications," *IEEE Transactions on Energy Conversion*, Vol. 26, No. 1, 73–82, Mar. 2011.
11. Chen, M., K.-T. Chau, C. H. T. Lee, and C. Liu, "Design and analysis of a new axial-field magnetic variable gear using pole-changing permanent magnets," *Progress In Electromagnetics Research*, Vol. 153, 23–32, 2015.
12. Uzhegov, N., J. Pyrhönen, and S. Shirinskii, "Loss minimization in high-speed permanent magnet synchronous machines with tooth-coil windings," *Proc. IEEE IECON*, 2960–2965, Nov. 2013.
13. Xu, G., L. Jian, W. Gong, and W. Zhao, "Quantitative comparison of flux-modulated interior permanent magnet machines with distributed and concentrated windings," *Progress In Electromagnetics Research*, Vol. 129, 109–123, 2012.
14. Lim, M.-S., S.-H. Chai, J.-S. Yang, and J.-P. Hong, "Design and verification of 150-krpm pmsm based on experiment results of prototype," *IEEE Transactions on Industrial Electronics*, Vol. 62, No. 12, 7827–7836, Dec. 2015.
15. Salonen, M. and M. Perttula, "Utilization of concept selection methods: A survey of finnish industry," *Proc. ASME IDETC/CIE*, 527–535, Sep. 2005.
16. Pyrhönen, J., V. Ruuskanen, J. Nerg, J. Puranen, and H. Jussila, "Permanent-magnet length effects in AC machines," *IEEE Transactions on Magnetics*, Vol. 46, No. 10, 3783–3789, Oct. 2010.
17. Uzhegov, N., J. Nerg, and J. Pyrhönen, "Design of 6-slot 2-pole high-speed permanent magnet synchronous machines with tooth-coil windings," *Proc. XXIst ICEM*, 2537–2542, Sep. 2014.
18. Borisavljevic, A., H. Polinder, and J. Ferreira, "On the speed limits of permanent-magnet machines," *IEEE Transactions on Industrial Electronics*, Vol. 57, No. 1, 220–227, Jan. 2010.
19. Zhao, W., M. Cheng, R. Cao, and J. Ji, "Experimental comparison of remedial single-channel operations for redundant flux-switching permanent-magnet motor drive," *Progress In Electromagnetics Research*, Vol. 123, 189–204, 2012.
20. Binder, A. and T. Schneider, "High-speed inverter-fed ac drives," *Proc. ACEMP'07 Int. Aegean Conf.*, 9–16, Sep. 2007.
21. Pugh, S., *Creating Innovative Products Using Total Design: The Living Legacy of Stuart Pugh*, edited by D. Clausing and R. Andrade, Addison-Wesley, New York, 1996.
22. Saaty, T. L., *The Analytic Hierarchy Process*, McGraw-Hill, New York, 1980.
23. Matzen, M., M. Alhajji, and Y. Demirel, "Chemical storage of wind energy by renewable methanol production: Feasibility analysis using a multi-criteria decision matrix," *Energy*, Vol. 93, 343–353, 2015.
24. Girones, V., S. Moret, F. Marechal, and D. Favrat, "Strategic energy planning for large-scale energy systems: A modelling framework to aid decision-making," *Energy*, Vol. 90, 173–186, 2015.
25. Thakker, A., J. Jarvis, M. Buggy, and A. Sahed, "3dcad conceptual design of the next-generation impulse turbine using the pugh decision-matrix," *Materials and Design*, Vol. 30, No. 7, 2676–2684, 2009.
26. Ullman, D. G., *The Mechanical Design Process*, McGraw-Hill, New York, 2010.
27. Okudan, G. and S. Tauhid, "Concept selection methods — A literature review from 1980 to 2008," *International Journal of Design Engineering*, Vol. 1, No. 3, 243–277, 2008.
28. Nasiri-Zarandi, R., M. Mirsalim, and A. Cavagnino, "Analysis, optimization, and prototyping of a brushless dc limited-angle torque-motor with segmented rotor pole tip structure," *IEEE Transactions on Industrial Electronics*, Vol. 62, No. 8, 4985–4993, Aug. 2015.
29. Dziadak, B. and A. Michalski, "Evaluation of the hardware for a mobile measurement station," *IEEE Transactions on Industrial Electronics*, Vol. 58, No. 7, 2627–2635, Jul. 2011.
30. Meyar-Naimi, H. and S. Vaez-ZAdeh, "Sustainability assessment of a power generation system using dsr-hns framework," *IEEE Transactions on Energy Conversion*, Vol. 28, No. 2, 327–334, Jun. 2013.

31. Chedid, R., H. Akiki, and S. Rahman, "A decision support technique for the design of hybrid solar-wind power systems," *IEEE Transactions on Energy Conversion*, Vol. 13, No. 1, 76–83, Mar. 1998.
32. Cogent, "Non-oriented electrical steel," [Online]. Available: http://cogent-power.com/, 2016.
33. Senda, K., M. Namikawa, and Y. Hayakawa, "Electrical steels for advanced automobiles — Core materials for motors, generators, and high-frequency reactors," *JFE Technical Report*, No. 4, 67–73, 2004.
34. Tarter, R. E., *Solid-state Power Conversion Handbook*, John Wiley & Sons, New York, NY, 1993.
35. Nasar, S. A. and L. E. Unnewehr, *Electromechanics and Electric Machines*, JohnWiley & Sons, New York, 1979.
36. Kolondzovski, Z., A. Belahcen, and A. Arkkio, "Comparative thermal analysis of different rotor types for a high-speed permanent-magnet electrical machine," *IET Electric Power Applications*, Vol. 3, No. 4, 279–288, Jul. 2009.
37. Clemens, S. L. and W. C. Faulkner, *Engineered Materials Handbook*, ASM, Metals Park OH, 1991.
38. Yon, J., P. Mellor, R. Wrobel, J. Booker, and S. Burrow, "Analysis of semipermeable containment sleeve technology for high-speed permanent magnet machines," *IEEE Transactions on Energy Conversion*, Vol. 27, No. 3, 646–653, Sep. 2012.
39. Uzhegov, N., E. Kurvinen, J. Nerg, J. Pyrhönen, J. Sopanen, and S. Shirinskii, "Multidisciplinary design process of a 6-slot 2-pole high-speed permanent-magnet synchronous machine," *IEEE Transactions on Industrial Electronics*, Vol. 63, No. 2, 784–795, Feb. 2016.